10.1515/tvsb-2017-0019

Transactions of the VŠB – Technical University of Ostrava

Civil Engineering Series, Vol. 17, No. 1, 2017

paper #19

Ondřej PEŠEK[1], Jindřich MELCHER[2]

SHAPE AND SIZE OF INITIAL GEOMETRICAL IMPERFECTIONS OF STRUCTURAL GLASS MEMBERS

Abstract

In this paper measuring and determining of initial geometrical imperfections of set of glass members are presented. Measured specimens had the different dimensions and different composition – monolithic glass or laminated glass using different types of interlayer foils and glass panes. The shape of initial overall bow was measured using different methods and results were statistically evaluated and compared with allowable values defined in standards.

Keywords

Structural glass, laminated glass, initial geometrical imperfections, normal distribution, log-normal distribution.

1 INTRODUCTION

Glass has been established as a material of load carrying members and structures in the end of twentieth century and its importance still grows [1]. Due to slender of glass members it is necessary to check them on stability problems – flexural or lateral torsional buckling or interaction of them. Design methods of steel and timber structures are not completely usable for glass structures because of several differences (initial imperfections, brittle behaviour and laminated glass behaviour) [2]. The shape and size of initial geometrical imperfections are poorly published in recent publications.

Behaviour of imperfect columns and beams under load was published in [3]. Equation (1) describe (according to the second order theory) dependency of deformation $f(w_0)_x$ of axially loaded imperfect column on amplitude of initial imperfection. Sinusoidal shape of overall bow (see Fig. 2) imperfection is considered. Flexural deformation increases with increasing amplitude of initial imperfection.

$$f\left(w_0\right)_x = w_0 \frac{N}{N_{\mathrm{cr}} - N} \cdot \cos \frac{\pi \cdot x}{L} \tag{1}$$

where:

w_0 – is amplitude of initial imperfection [mm],

N – axial force [N],

N_{cr} – Euler's critical force [N],

L – column (buckling) length [mm] and

x – point of interest, distance from mid-span [mm].

[1] Ing. Ondřej Pešek, Department of Metal and Timber Structures, Faculty of Civil Engineering, Brno University of Technology, Veveří 331/95, 602 00 Brno, Czech Republic, phone: (+420) 541 147 329, e-mail: pesek.o@fce.vutbr.cz.

[2] Prof. Ing. Jindřich Melcher, DrSc., Department of Metal and Timber Structures, Faculty of Civil Engineering, Brno University of Technology, Veveří 331/95, 602 00 Brno, Czech Republic, phone: (+420) 541 147 300, e-mail: melcher.j@fce.vutbr.cz.

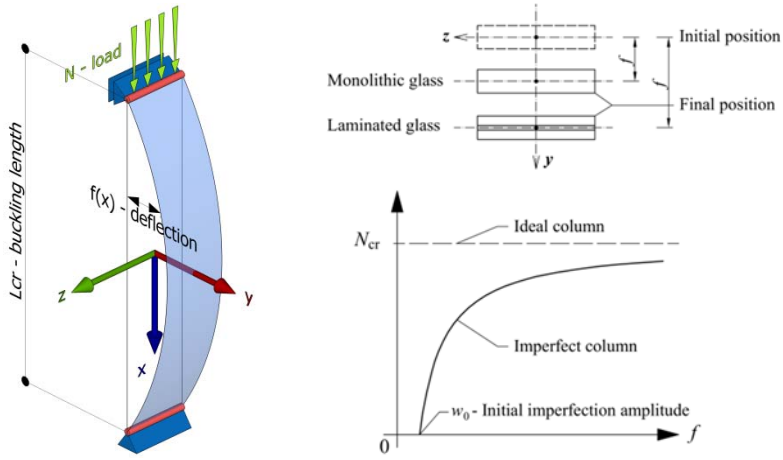

Fig. 1: Flexural buckling of glass column, load-deflection curve of perfect and imperfect member

2 METHODOLOGY

Three types of initial imperfections are distinguished according to their origin: geometrical imperfections (geometrical curvature of beam or column), construction imperfections (actual point of load application etc.) and physical imperfections (residual stresses, inhomogeneity of the material). Only geometrical imperfections are relatively easily measurable and observable before placing the member in the structure.

2.1 Geometrical imperfections of glass members and normative documents

The differences of nominal dimensions are generated during manufacturing processes and they should be lower than limits specified in product standards. Following tolerances should be checked: (i) glass pane thickness, (ii) glass pane length, wide and rectangularity, (iii) edge deformations due to vertical production (does not apply on float glass) and (iv) planarity (flatness).

Geometrical deformations (curvature) results from glass tempering processes (manufacturing process of fully tempered glass or heat strengthened glass). The size of deformations depends on type of glass (coated glass, patterned glass etc.), on glass dimensions and aspect ratio, on nominal thickness and on type of tempering process (vertical or horizontal).

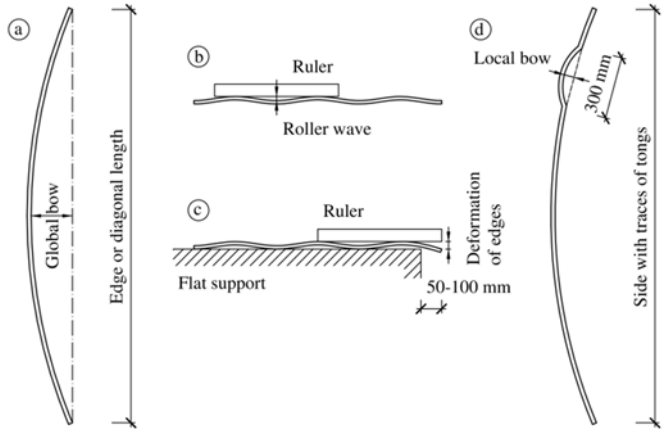

Fig. 2: Glass pane deformations types

Four types of deformations are: (a) overall bow, (b) roller wave (only for horizontally tempered glass), (c) curvature of edges (only for horizontally tempered glass) and (d) local bow (only for horizontally tempered glass) – see Fig. 2.

The maximum allowable values of the overall bow deflection according to the EN 1863-1 [6] and EN 12150-1 [7] are: (i) 3.0 mm/m for float glass horizontally tempered, (ii) 4.0 mm/m for horizontally tempered glass (other types) and (iii) 5.0 mm/m for vertically tempered glass (all types).

Tab. 1: List of maximum allowed imperfections according to the EN 1863-1 [6] and EN 12150-1 [7]

Glass type	Position at tempering	FTG or HSG glass	
		Global bow mm/m	Local bow mm/300 mm
Float glass without coating	Horizontal	3.0	0.3
Others	Horizontal	4.0	0.5
All	Vertical	5.0	1.0

2.2 Specimens

Initial geometrical imperfections (global bow) were measured on specimens listed in Table 2.

Tab. 2: List of specimens

Type of glass	Description	Dimensions [mm]			Measuring device	Pcs.
		Length	Width	Thick.		
ESG 12	Safety glass	1500	150	12	Carl Zeiss	3
VG 66.2	Laminated glass with PVB foil	1500	150	6+6	Carl Zeiss	3
VSG 66.2	Laminated safety glass with EVASAFE foil	1500	150	6+6	Carl Zeiss	6
VSG 444.33	Laminated safety glass with EVASAFE foil	1500	150	4+4+4	Carl Zeiss	3
VG 1010.2	Laminated glass with EVA foil	2400	280	10+10	own	3
VG 88.2	Laminated glass with PVB foil	2400	280	8+8	own	3
VG 66.2	Laminated glass with PVB foil	2400	280	6+6	own	3
VSG 88.2	Laminated safety glass with EVASAFE foil	2000	200	8+8	own	3
VG 88.2	Laminated glass with PVB foil	2000	200	8+8	own	6
					Sum	**33**

Overall bow shape of glass specimens was analysed using three devices: laser scan; mechanical measuring system Carl Zeiss and measuring device of own construction. Measured specimen was fixed in vertical position (due to dead load deflections elimination) and supported by two timber blocks according to EN 1863-1 and EN 12150-1. Permanent stability of glass was ensured by steel stand.

2.3 Laser scanning with FARO 3D

An actual shape of glass member was measured with laser scan device FARO Focus3D 120 (SN: LLS061304311). Some laser rays go throw glass panes. Any types of coating providing better reflex properties were used, but result still wasn't satisfying. From this reason different measuring methods were used afterwards.

2.4 Carl-Zeiss measurement device

Measuring device Carl Zeiss was composed from height-adjustable guiding rail situated on two supporting threaded columns, which were independently height-adjustable by two locking screws. Wagon with mechanical deflection sensor (Carl Zeiss 003 19 with accuracy 0.01 mm) was moving on guiding rail (x axis). Wagon was able to move with mechanical indicator in vertical (z

axis) and lateral (y axis) direction. Measuring set up was tuned so that the tip of indicator watches was situated 10 mm under measured specimen edge. Measuring set up is plotted in Fig. 3a.

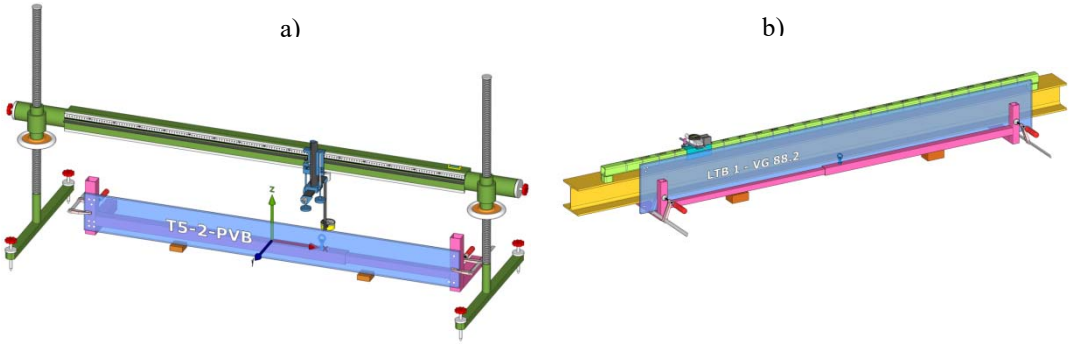

Fig. 3: Measurement set-up with a) Carl-Zeiss equipment and b) own construction equipment

2.5 Own construction measurement device

Carl-Zeiss device was usable only for specimens up to length 1500 mm. For measuring of longer specimens own construction of measurement device inspired by the research at Ghent University [4] was designed and manufactured.

Device was composed of horizontal beam (HEA160) and guiding rail (SHS 50/50/4). Wagon (SHS 60/60/4) carried digital gauge Mitutoyo Absolute Digimatic ID-C with accuracy 0.01 mm – see Fig. 3b.

2.5 Measuring Device Imperfection

Because of elimination of measurement errors due to measuring set up geometrical imperfections (guiding rail) every specimen and both its edges were measured in two locations (positive location and negative location) and in two positions (position 1 and position 2). Lateral horizontal deflection (y coordinate) was measured in steps of 50 mm. Both edges were measured two times for both locations and positions of specimen.

In the first step of evaluation the measured coordinates were transferred to new coordinate system, so that coordinate $y = 0$ at both ends of specimen. In the second step the average coordinates were made from two measuring – to received coordinates of deflections (imperfections) $u_{0,\mathrm{uncorr}}(x)$. In the last step the evaluated deflections were corrected by the value of guiding rail imperfections.

Measuring set up itself was subjected to implicit errors – precision of mechanical deflection device, deviations of the theoretical parallel placement of specimen and test set up and geometrical imperfections of the guiding rail. The first two kinds of errors are not significant and were not taken into account. Errors due to shape imperfections of the guiding rail were significant and they were taken into account by compensating method described in Fig. 4.

The geometrical imperfection of the guiding rail was deducted from measuring the initial shape imperfections of the same glass specimen twice: once in the conventional position ($u_{0,\mathrm{uncorr},1}$) and once in the mirrored position ($u_{0,\mathrm{uncorr},2}$).

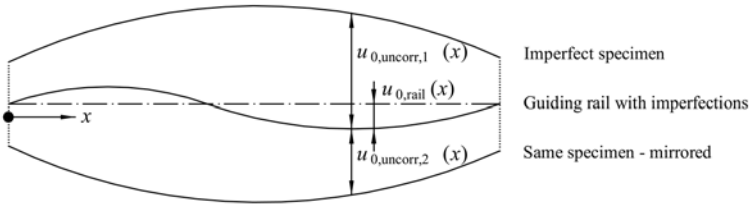

Fig. 4: Determination of guiding rail imperfections

Using this principle, the shape of imperfection of the guiding rail $u_{0,\mathrm{rail}}(x)$ was determined with (2). Repeating this process several times, the imperfections of the guiding rail could be reproduced with high accuracy. The resulting corrected geometrical imperfection $u_0(x)$ was obtained using (3).

$$u_{0,\mathrm{rail}}(x) = \frac{u_{0,\mathrm{uncorr},1}(x) - u_{0,\mathrm{uncorr},2}(x)}{2} \tag{2}$$

$$u_0(x) = u_{0,\mathrm{uncorr}}(x) \pm u_{0,\mathrm{rail}}(x) \tag{3}$$

Shapes of imperfections of the guiding rail are plotted in Fig. 5 for both measuring devices. To evaluation of initial imperfections of all specimens the mean value of guiding rail imperfections was taken into account. The shape of initial imperfections from all measuring is similar, but on the other hand the amplitudes are relatively different.

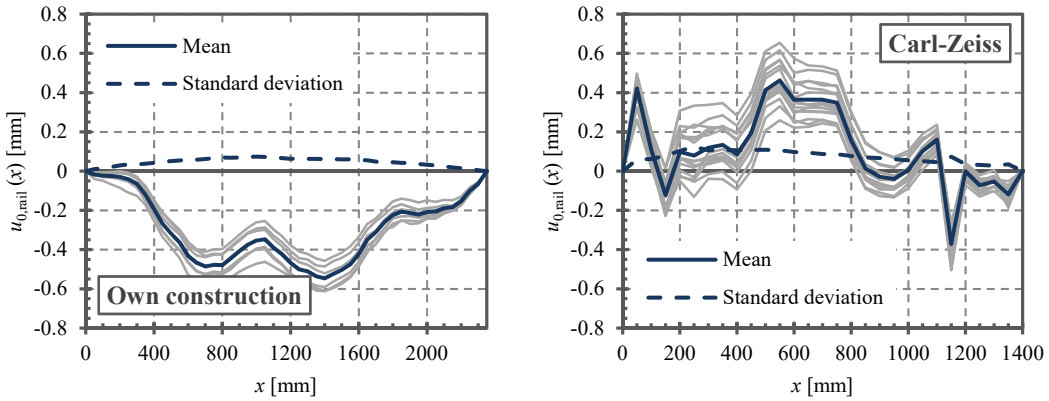

Fig. 5: Measured shapes of measurement devices

3 RESULTS AND DISCUSSION

Evaluation of the measurement was carried out according to the approach presented by Belis et al. [4]. Imperfections of all specimens are evaluated with positive sign.

2.5 Overall bow shape and size

The value of initial imperfection u_0/L is representing maximum relative amplitude, which is not generally situated in the half of length of specimen. Relative imperfection amplitudes are plotted in Fig. 6 according to the glass type. Mean value is 0.42 mm/m and maximum value is 1.6 mm/m that is much lover than allowable values (Tab. 1)

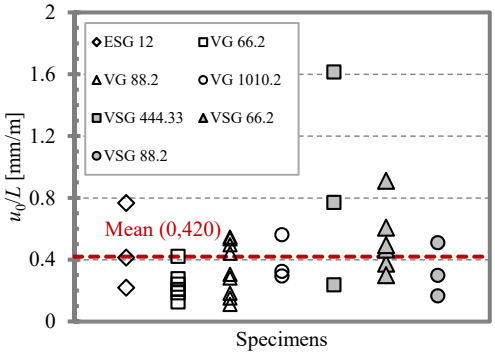

Fig. 6: Relative amplitudes of initial imperfections of tested specimens

Graph in Fig. 7 shows actual shapes of glass member measurements. Curves are coloured according to the glass type. On horizontal axis length of specimens is plotted in relative units.

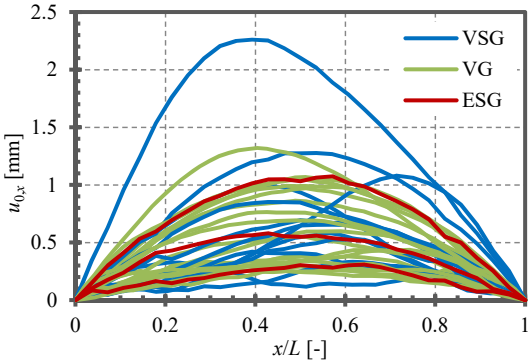

Fig. 7: Imperfect shapes of glass rods

From imperfection shapes plotted in Fig. 7 it is clear that initial imperfection shape should be approximated by second order parabola (4) or half sinusoidal wave (5):

$$a^{\mathrm{par}}(x) = u_0 - \frac{u_0}{(0{,}5 \cdot L)^2} \cdot x^2 \tag{4}$$

$$a^{\sin}(x) = u_0 \cdot \cos\left(\frac{\pi \cdot x}{L}\right) \tag{5}$$

Overall bow shapes of typical (most of the samples) and untypical (only unique case) specimens are plotted in Fig. 8. In the graph the approximation curves (sinusoidal and parabolical) are plotted. On secondary vertical axis there is plotted error of approximations.

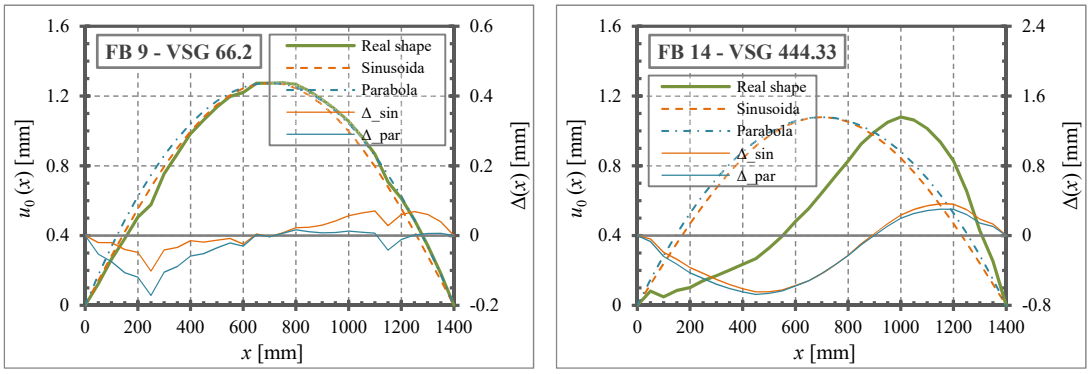

Fig. 8: Examples of typical (FB9) and untypical (FB14) shapes of imperfections

To quantitatively describe the approximation quality of the initial imperfection shape, a fitting error (fe^{par} for the parabola and fe^{sin} for the sinusoid) is defined as the ratio of the maximal error (Δ^{par} for the parabola and Δ^{sin} for the sinusoid) and the maximal initial imperfection u_0 (6) and (7).

$$fe^{\mathrm{par}} = \Delta^{\mathrm{par}} / u_0 \cdot 100 \tag{6}$$

$$fe^{\sin} = \Delta^{\sin} / u_0 \cdot 100 \tag{7}$$

The error of approximation at position x is defined by (8) and (9).

$$\Delta^{\mathrm{par}}(x) = u_0(x) - a^{\mathrm{par}}(x) \tag{8}$$

$$\Delta^{\sin}(x) = u_0(x) - a^{\sin}(x) \tag{9}$$

The values of fitting errors fe^{par} and fe^{sin} are plotted in graphs in Fig. 9.

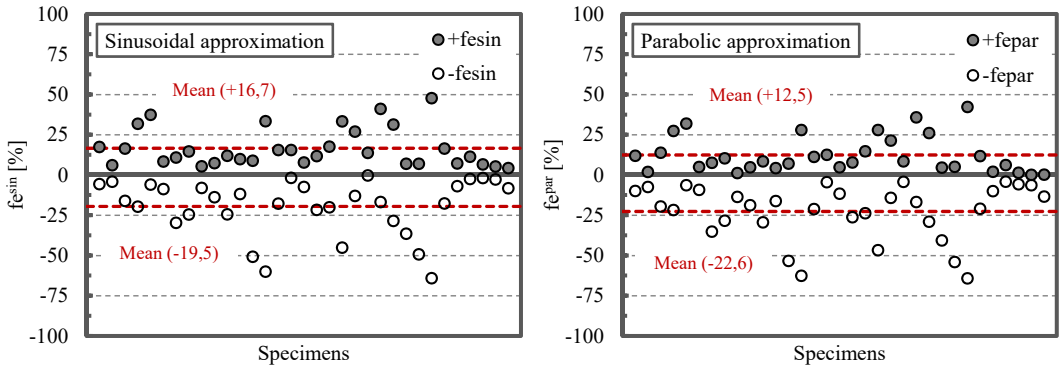

Fig. 9: Fitting errors for sinusoidal and parabolic approximation

The mean value of the positive fitting error for a sinusoidal approximation (+16.7 %) is higher than for parabolic approximation (+12.5 %). In the case of negative fitting error it is opposite: parabola (-22.6 %) and sinusoid (-19.5 %). Adding and subtracting of absolute values of fitting errors for parabolic approximation (12.5 + 22.6 = 35.1 % or 22.6 – 12.5 = 10.1 %) and sinusoid approximation (16.7 + 19.5 = 36.2 % and 19.5 – 16.7 = 2.8 %) leads to the conclusion, that the sinusoidal approximation is more stable. Both functions can be used for implementing initial imperfections in numerical models. However, preference is given to the sinusoidal function because it is corresponding to the eigen-mode, which is often adopted as initial geometrical imperfection in buckling analysis.

3.1 Influence of variable parameters on imperfection size

Specimen geometry. In Fig. 11 ratio L/W is plotted on the horizontal axis, where L is glass member length and W is section modulus on weak axis. On vertical axis relative amplitudes of imperfections are plotted. From graph in Fig. 11 could be said that relative overall bow increases with increasing geometry ratio L/W, but this phenomenon is probably caused by small and non-representative set of specimens. Research carried out by Belis et al. [4] on much larger set of specimens (there were more than 500 specimens) shows, that geometry ratio L/W has no influence on geometrical imperfections.

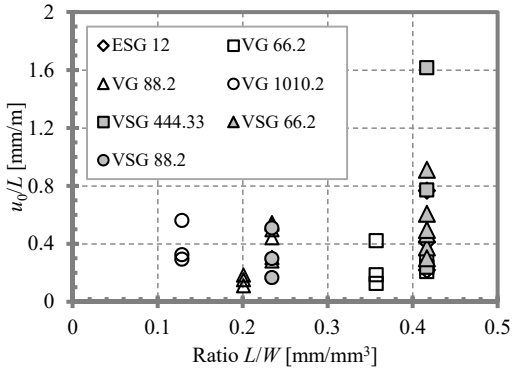

Fig. 11: Influence of ration L/W on imperfections size

Glass tempering. Influence of glass tempering on overall bow imperfection amplitudes is plotted in graphs in Fig. 12. Fig. 12 shows that float annealed glass imperfections (mean value for ANG is 0.317 mm/m) are smaller than those for the fully tempered glass (mean value for FTG is 0.544 mm/m).

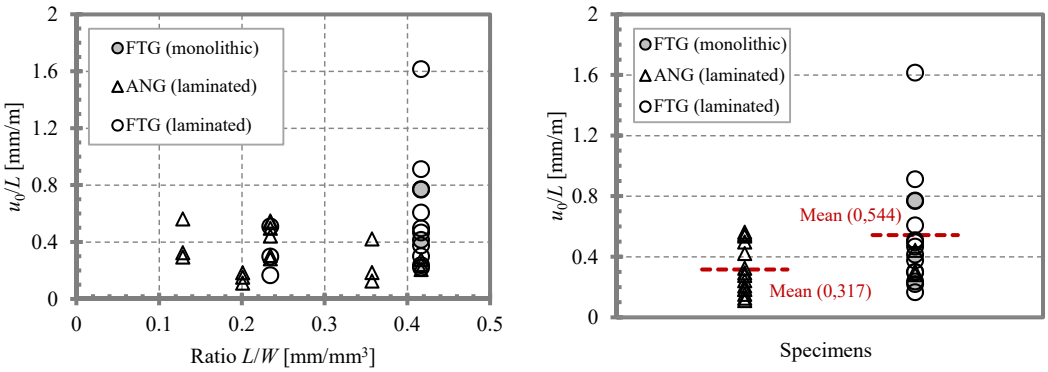

Fig. 12: Influence of glass tempering on imperfections size

Glass laminating. Influence of glass laminating on overall bow imperfection amplitudes is plotted in graphs in Fig. 13. Fig. 13 shows that monolithic glass imperfections (mean value is 0.468 mm/m) are similar as for laminated glass (mean value is 0.415 mm/m). Glass laminating has not significant influence on imperfection size. Ghent university research [4] showed that imperfections are rather influenced by used laminating technology and technique.

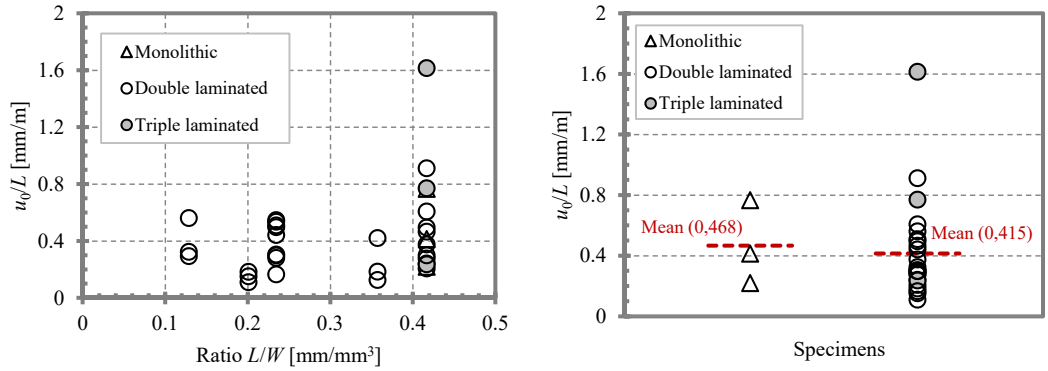

Fig. 13: Influence of glass laminating on imperfections size

Interlayer material. Influence of interlayer material on imperfection amplitudes is plotted in graphs in Fig. 14. Fig. 14 shows that laminated glass with PVB foil has significantly lower imperfections (mean value 0.302 mm/m) than laminated glass with EVASAFE foil (mean value 0.529 mm/m). But this difference is caused by usually used combinations of glass and interlayer material - ANG glass is usually laminated with PVB foil and FTG glass is used with EVASAFE foil.

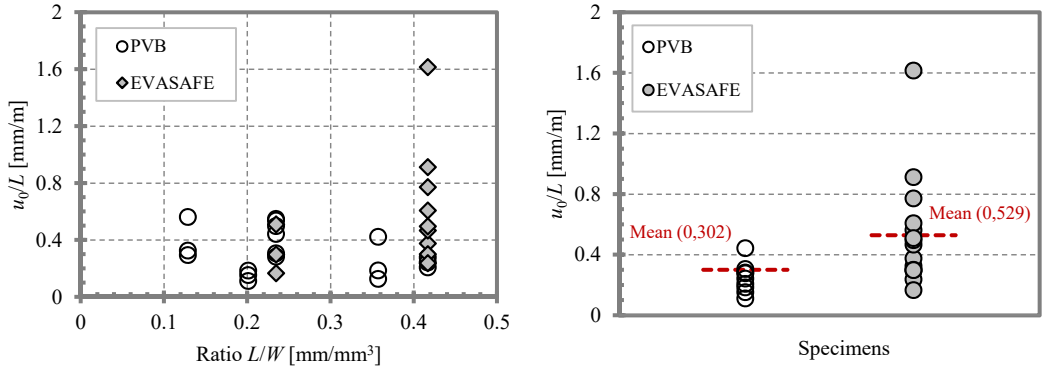

Fig. 14: Influence of interlayer material on imperfections size

3.3 Characteristic value of initial imperfections

For practice design it is necessary to know the characteristic value of initial imperfection $(u_0/L)_k$, which is entering into buckling analysis. Generally, characteristic value is considered as 5% quantile.

The results of initial imperfections measuring were evaluated such that all imperfection values were positive. Actually the curvature might be convex or concave and mean value of large population is theoretically equal to zero.

Available data set of 33 absolute values is assumed as truncated normal distribution with truncation at zero, in agreement with the Probabilistic Model Code [5] by JCSS (The Joint Committee on Structural Safety). This truncated normal distribution is equivalent to a normal distribution which corresponds to a modified population. More specifically, the available data set was considered twice, whereas one time it was given a negative sign and for the other it kept a positive sign. Consequently, a new population of 66 imperfections values was obtained with a mean equal to zero and with normal distribution - Fig. 15 on the left. For new population the characteristic value was calculated.

In general, 5% quantile is calculated by (10), where μ is mean value and σ is standard deviation.

$$5\%\ \text{quantile} = \mu + 1.645 \cdot \sigma \tag{10}$$

Because of a "doubled" population (to get correct data set), 2.5% quantile on each tail of the normal distribution was calculated using (11):

$$5\%\ \text{quantile}_{\text{truncated distribution}} = 2.5\%\ \text{quantile}_{\text{untruncated distribution}} = \mu + 1.96 \cdot \sigma \tag{11}$$

An alternative approach is to analyse directly the asymmetric probability density function based on original 33 imperfection measurement values only. Histogram of original data set with log-normal distribution function is illustrated in Fig 15 on the right. Characteristic value (5% quantile) was calculated by STATISTICA software [8].

Characteristic values of initial imperfections were calculated for annealed glass, fully tempered glass and for both types together using both methods presented above. Results of statistical evaluation are listed in Tab. 3. The similar values (differences are from 5 % to 7 %) resulting from both methods show their rightness.

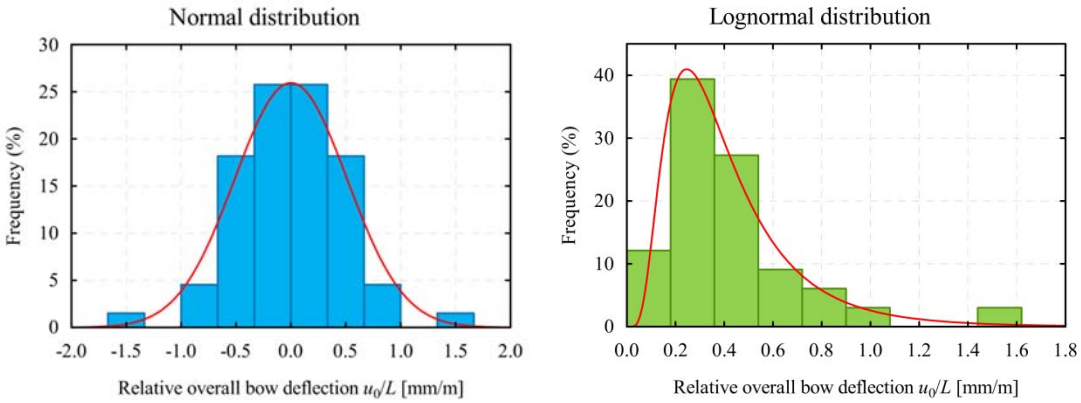

Fig. 15: Histograms of relative overall bow deflections

Characteristic value for annealed glass $(u_0/L)_k$ = 0.69 mm/m (limit value is not prescribed), for fully tempered glass $(u_0/L)_k$ = 1.297 mm/m (limit value is 3 mm/m for horizontal tempering). It means that limits in standards are not exceeded. Calculated values correspond to the relative imperfections L/1400 and L/800 respectively.

Tab.3: Results of statistical evaluation

Glass type	Pcs	Statistical distribution			
		Normal		Lognormal	
Float annealed	18	0.693	36 realizations	0.652	18 realizations
Fully tempered	15	1.297	30 realizations	1.230	15 realizations
Both together	33	1.004	66 realizations	0.936	33 realizations

4 CONCLUSIONS

This paper summarizes results of measuring of laminated glass members geometrical imperfections. The great influence on overall bow imperfection amplitudes has glass tempering process, other influences are negligible. The main result – characteristic value of initial geometrical overall bow shape is much less than limit value described by standards. Results show that actual shape of glass specimens could be approximated by sinusoidal wave.

ACKNOWLEDGMENT

This paper has been elaborated within the support of the Projects of Czech Ministry of Education, Youth and Sports on Faculty of civil engineering, Brno University of Technology No FAST-S-17-4655.

LITERATURE

[1] HALDIMANN, M., LUIBLE, A., OVEREND, M. *Structural Use of Glass*. Zurich: ETH Zurich, 2008. ISBN 3-85748-119-2.

[2] PEŠEK, O., MELCHER, J., HORÁČEK, M.: *Experimental Verification of the Buckling Strength of Structural Glass Columns*. In Procedia Engineering, Volume 161, 2016, pp. 556-562, ISSN 1877-7058, doi:10.1016/j.proeng.20106.08.691.

[3] BŘEZINA, V. *Buckling Load Capacity of Metal Rods and Beams* (Vzpěrná únosnost kovových prutů a nosníků). Prague: Czechoslovak Academy of Science, 1962.

[4] BELIS, J., MOCIBOB, D., LUIBLE, A., VANDEBROEK, M. On the size and shape of initial out-of-plane curvatures in structural glass components. *Elsevier Ltd., Construction and Building Materials*. 2011, vol. 25, Issue 5, pp. 2700-2712. ISSN: 0950-0618.

[5] *JCSS probabilistic model code*. The joint committee on structural safety [online]. 2001 [cit. 2014-12-15]. Available from: https://www.jcss.byg.dtu.dk.

[6] *EN 1863-1. Glass in building – Heat strengthened soda lime silicate glass – Part 1: Definition and description*. European Committee for Standardization, Brussel. ref. number EN 1863-1:2011 E.

[7] *EN 12150-1. Glass in building – Thermally toughened soda lime silicate glass – Part 1: Definition and description*. European Committee for Standardization, Brussel. ref. number EN 12150-1:2000 E.

[8] *StatSoft Inc. STATISTICA © Cz 12*, [software]. Available from: https://www.statsoft.com.